Supporting Information

Mitochondrial Imaging with Combined Fluorescence and Stimulated Raman Scattering Microscopy using a Probe of Aggregation-Induced Emission Characteristic

Xuesong Li,[†,∥,§] Meijuan Jiang,[‡,§] Jacky W. Y. Lam,[‡] Ben Zhong Tang,[*,‡] and Jianan Y. Qu[*,†,∥]

[†]*Department of Electronic and Computer Engineering, Hong Kong University of Science and Technology, Clear Water Bay, Kowloon, Hong Kong, China*

[∥]*Center of Systems Biology and Human Health, School of Science and Institute for Advanced Study, Hong Kong University of Science and Technology, Clear Water Bay, Kowloon, Hong Kong, China*

[‡]*Department of Chemistry, Hong Kong Branch of Chinese National Engineering Research Center for Tissue Restoration and Reconstruction, and Division of Biomedical Engineering, Hong Kong University of Science and Technology, Clear Water Bay, Kowloon, Hong Kong, China*

[§] *The authors contributed equally.*

[*] *Correspondence email: tangbenz@ust.hk (Tang, B.Z.) and eequ@ust.hk (Qu, J.Y.)*

Equipment setup for FL-SRS system

In stimulated Raman scattering (SRS) imaging, a pump-laser-integrated Optical Parametric Oscillator (OPO), also known as one-box OPO (*pico*Emerald S; Applied Physics & Electronics, Berlin, Germany), was used as the light source for both pump and Stokes beams. In brief, *pico*Emerald S provides an output pulse train at 1,031 nm with 2.1-ps pulse duration and 80-MHz repetition rate, which serves as the Stokes beam. The double-frequency beam at 516 nm was used to seed an OPO to produce a mode-locked pulse train with 1.9-ps pulse duration synchronously. The synchronized pump beam was continuously tunable from 780 nm to 960 nm while the Stokes beam was fixed at 1,031 nm. The intensity of the 1,031 nm Stokes beam was modulated by a built-in electro-optical modulator (EOM) at 20 MHz driven by a sinusoidal wave function generator with a modulation depth of more than 95% to achieve shot-noise limited detection sensitivity. The pump beam was spatially overlapped with the Stokes beam with a dichroic mirror inside *pico*Emerald S. The temporal overlap between Pump and Stokes pulse trains was ensured with a built-in delay stage and optimized with 6-μm polystyrene beads (Polysciences, Inc., Warrington, PA), pure glycerol, heavy water (99% pure, D_2O) and EdU (10 mM in PBS solution) based on their specific Raman peaks. The 4 different materials make sure that optimization of the temporal overlapping covers the fingerprint, cell-silent and carbon-hydrogen (C-H) vibration regions in the Raman spectrum.

In the two-photon excited fluorescence (TPEF) imaging modality, a femtosecond Ti:sapphire laser with a 140-fs pulse duration (Chameleon Ultra II, Coherent, Santa Clara, CA) was tuned at 780 nm and used as the two-photon excitation beam. Both ps (SRS) and fs (TPEF) beams were collimated by a pair of achromatic doublets and magnified to match the 3-mm galvanometric scanners (6215H, Cambridge Technology), respectively. A superachromatic half-wave plate (SAHWP05M-1700, Thorlabs) was used to rotate the fs beam from horizontal to vertical polarization direction after collimation. Then the SRS and TPEF beams were combined by a polarizing beam splitter (CCM1-PBS252/M, Thorlabs) and coupled into a home-made upright laser-scanning microscope. The combined beams were firstly directed into a telecentric scan lens (SL50-CLS2, Thorlabs) and then through an infinity corrected tube lens (TTL200-B-SP, Thorlabs). A water immersion objective (UAPO40XW3/340, 1.15 NA, Olympus) with high near-IR transmission was used to focus the excitation beams into the examined samples and collect the backscattered TPEF signals.

The pump/Stokes/TPEF beam sizes were matched to fill the back aperture of the objective. A dichroic mirror (FF665-Di02, Semrock) was placed above the objective to reflect the TPEF signals to the detection system. The TPEF signals were relayed by a telescope to a hybrid photomultiplier tube (PMT) detector and a time-correlated single photon counting (TCSPC) module (HPM-100-40 and SPC-150, Becker & Hickl GmbH) was used to record the TPEF photon counts. A short-pass filter (E740sp, Chroma) was

used to reject the reflected excitation beam and the fluorescence signal was further purified by a band-pass filter (ET510/30m, Chroma).

The forward-going pump and Stokes beams after passing through the sample were collected in transmission with a high N.A. oil immersion condenser (UAAC, Achromat/aplanat condenser, 1.4 N.A., Olympus, Tokyo, Japan) following Köhler illumination. A telescope system consisting of a pair of achromatic doublets was then used to image the scanning mirrors onto a large area (10 × 10 mm) Si photodiode (S3590-08; Hamamatsu) to descan beam motion during laser scanning. The photodiode was reversed bias by 51 V power supply to increase the saturation threshold. A high optical density (OD) short-pass filter (86108 shortpass at 975nm OD4, Edmund Optics) and band-pass filter (FF01-850/310, SRS imaging emission filter, Semrock) were used to block the Stokes beam completely and transmit the pump beam only. The output current of the photodiode was then fed into a radio frequency lock-in amplifier (A.P.E., Berlin, Germany) for highly sensitive and extremely fast detection with integration times down to below 100 ns. The time constant was set at 20 μs for the experiment and can be further decreased for other significant SRS signals detection other than alkyne bond. For imaging, 512 × 512 pixels were acquired for one frame with a 25.6-μs of pixel dwelling time and 20 μs of time constant from the lock-in amplifier (LIA). The amplitude output of the LIA was fed back into an acquisition card (PCIe-6363, National Instruments, Austin, TX) to reconstruct the image. The whole hardware were controlled by a home-built C# program which also gave synchronization signals to the scanners and TCSPC.

Laser powers after the 40× IR objective used for cell imaging are as follows: 30 mW for the pump beam; 100 mW for the modulated Stokes beam of 2,223 cm^{-1}, 2,160 cm^{-1}, 2,125 cm^{-1}, 2,065 cm^{-1} and 752 cm^{-1}; and 50 mW for the Stokes beam of 2,950 cm^{-1} and 2,845 cm^{-1} channels. For TPEF imaging, the 780-nm laser at the sample was controlled as low as 4 mW to exclude any possible photodamage and photobleaching. Similar to SRS imaging, the integration time of TPEF was also within 8 seconds for one frame.

For the hyperspectral SRS sweeping mode in solution, the pump beam wavelength of the *pico*Emerald S was sequentially tuned by the program through serial communication. For the alkyne SRS imaging, we adjusted the Lyot filter inside the laser (while fixing the OPO crystal temperature), and a pair of "alkyne-on" and "alkyne-off" images could be acquired within 3 seconds tuning time to avoid movement of the cells. The final alkyne SRS image was obtained by subtracting the on-resonant signals with off-resonant signals after imaging session. This method is called "intensity modulated SRL (IM-SRL)" to suppress the non-Raman backgrounds, including cross-phase modulation (XPM), transient absorption (TA) and thermal lensing effects, for they could severely deteriorate the genuine SRS signals especially in fingerprint and cell-silent vibration regions.

Synthesis of AIE-SRS-Mito

4-(Phenylethynyl)benzaldehyde was commercial available and was synthesized via Sonogashira reaction according to literature. ^{1}H NMR (400 MHz, DMSO-d_6) δ (ppm) 10.04 (s, 1H), 7.96 (d, 2H, J = 8.0 Hz), 7.78 (d, 2H, J = 8.0 Hz), 7.63–7.60 (m, 2H), 7.47–7.46 (m, 3H).

Synthesis of compound **3**: Into a 100 mL round bottom flask were dissolved 4-(phenylethynyl)benzaldehyde (206 mg, 1 mmol) and 4-bromophenylacetonitrile (196 mg, 1 mmol) in 40 mL ethanol. Sodium hydroxide (100 mg) was added. After stirring for 5 h at 50 ^{o}C, the pale yellow precipitates were filtered and washed with cold ethanol. The product was dried and weighted. Yield: 95 %. ^{1}H NMR (400 MHz, DMSO-d_6), δ (ppm): 8.13 (s, 1H), 8.00 (d, 2H, J = 8.0 Hz), 7.74–7.71 (m, 6H), 7.60–7.58 (m, 2H), 7.46–7.45 (m, 3H). ^{13}C NMR (100 MHz, DMSO-d_6), δ (ppm): 142.4, 133.6, 133.0, 132.1, 131.9, 131.5, 129.5, 129.2, 128.8, 127.9, 124.4, 122.8, 121.9, 117.5, 109.8, 91.8, 89.0. MS (MALDI-TOF): calculated for **3** ($C_{23}H_{14}BrN$): 383.0310, found: 383.0309.

Synthesis of compound **2**: Into a 100 mL two-necked round bottom flask equipped with a condenser were added **3** (192 mg, 0.5 mmol), 4-pyridinylboronic acid (74 mg, 0.6 mmol), potassium carbonate (172 mg, 1.25 mmol) and $Pd(PPh_3)_4$ (10 mg, 0.01mmol) in 10 mL and 3 mL water under nitrogen. The mixture was stirred and heated to reflux overnight. After cooling to room temperature and solvent evaporation, the mixture was extracted with dichloromethane (DCM) for three times. The organic phase was collected, washed with water and dried over anhydrous magnesium sulfate. After solvent evaporation, the crude product was purified by silica-gel column chromatography using DCM/MeOH as eluent. Yield: 99 %. ^{1}H NMR (400 MHz, $CDCl_3$), δ (ppm): 8.71 (d, 2H, J = 4.4 Hz), 7.93 (d, 2H, J = 8.4 Hz), 7.82 (d, 2H, J = 8.4 Hz), 7.74 (d, 2H, J = 8.4 Hz), 7.63 (d, 2H, J = 8.4 Hz), 7.60–7.54 (m, 5H), 7.39–7.36 (m, 3H).^{13}C NMR (100 MHz; $CDCl_3$), δ (ppm): 150.7, 147.3, 141.9, 139.2, 135.3, 133.3, 132.3, 132.0, 129.6, 129.0, 128.7, 127.9, 127.0, 126.1, 123.0 121.7, 117.9, 111.4. MS (MALDI-TOF): calculated for **2** ($C_{28}H_{18}N_2$): 382.1470, found: 382.1467.

Synthesis of AIE-SRS-Mito (**1**): Into a 100 mL two-necked round bottom flask were dissolved **2** (100 mg, 0.26 mmol) in 10 mL acetonitrile. Iodoethane (0.1 mL, 1.25 mmol) was then added and the mixture was heated to reflux overnight. After cooling to room temperature, 20 mL diethyl ether was added in portions. The yellow precipitates formed were filtered and washed with diethyl ether. The precipitates were redissolved in acetone and mixed with saturated NaPF6 solution (5 mL). After stirring for 1 h, acetone was evaporated. The light-yellow precipitate was filtered again, washed with water dried under reduced pressure. Yield: 70 %. ^{1}H NMR (400 MHz, DMSO-d_6), δ (ppm): 10.35 (s, 1H), 8.75 (d, 1H, J = 8.8 Hz), 8.30–8.26 (m, 2H), 7.73 (d, 1H, J = 8.0 Hz), 7.60–7.42 (m, 9H), 7.30–7.24 (m, 5H), 7.10 (d, 1H, J = 8.0 Hz), 4.43 (t, 2H, J = 7.2

Hz), 4.01(s, 3H) 1.89–1.84 (m, 2H), 0.82(t, 3H, J = 7.2 Hz). ^{13}C NMR (100 MHz, DMSO-d_6), δ (ppm): 153.3, 144.6, 143.6, 137.0, 134.0, 133.5, 131.9, 131.5, 129.7, 128.9, 126.9, 124.7, 124.5, 121.8, 117.5, 109.7, 92.1, 89.0, 55.6, 16.3. ^{31}P NMR (162 MHz, DMSO-d_6), δ (ppm): -131.0, 135.4, 139.8, 144.2, 148.6, 153.0, 157.4. ^{19}F NMR (376 MHz, DMSO-d_6), δ (ppm): -69.2, 71.0. MS (MALDI-TOF): calculated for cation of AIE-SRS-Mito ($C_{30}H_{23}N_2^+$): 411.1856, found: 411.1860. MS (MALDI-TOF): calculated for cation of AIE-SRS-Mito (PF_6^-): 144.9647, found: 144.9639.

Supplementary Figures and Tables

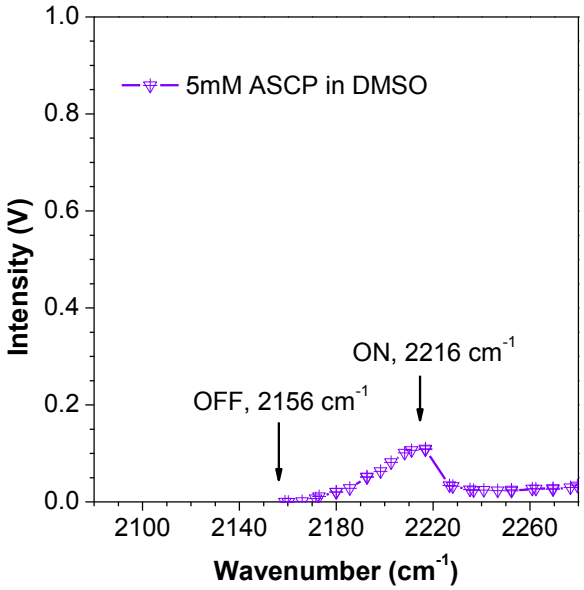

Figure S1. SRS spectrum of 5 mM ASCP in DMSO.

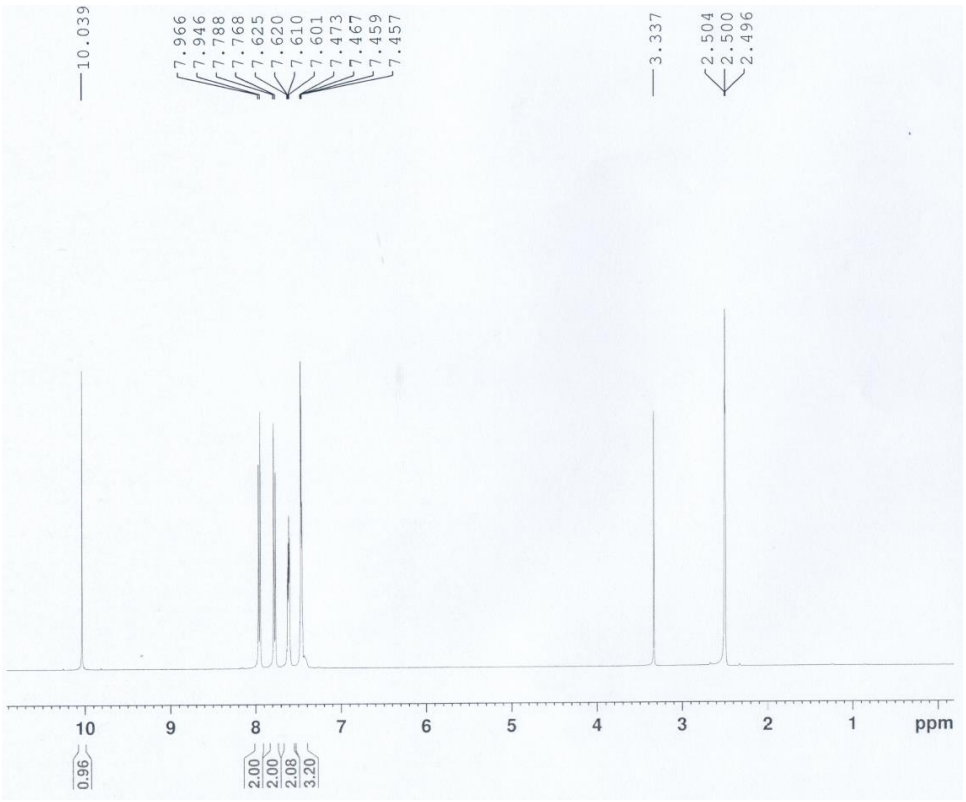

Figure S2. ^{1}H NMR spectrum of 4-(phenylethynyl)benzaldehyde in DMSO-d_6.

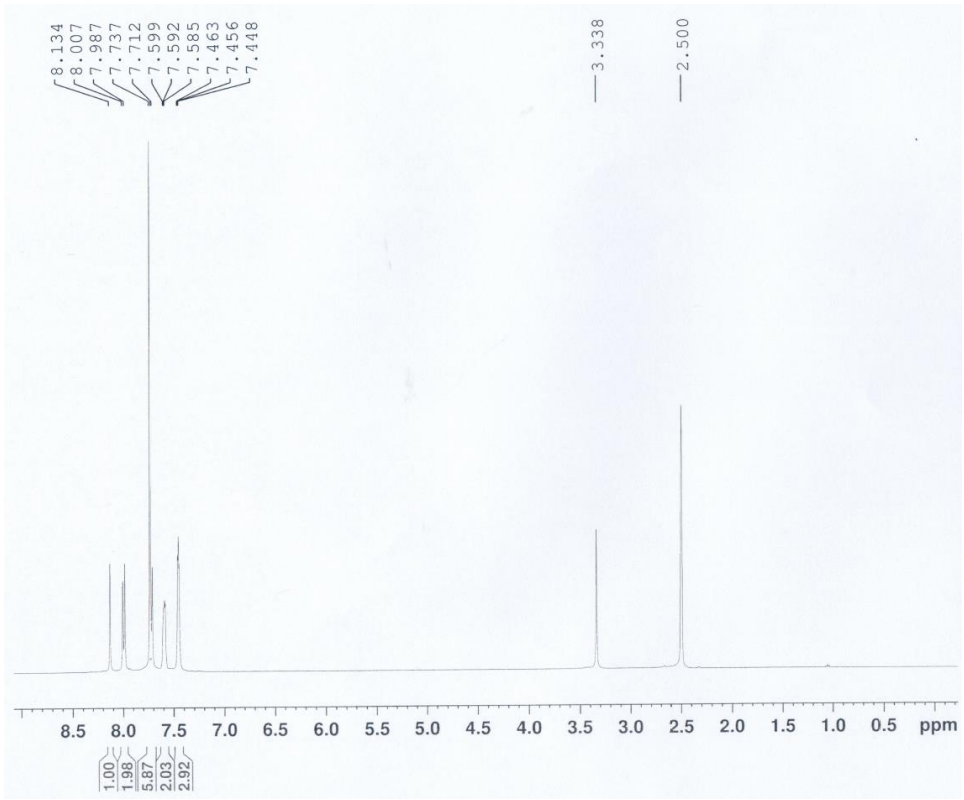

Figure S3. ^{1}H NMR spectrum of **3** in DMSO-d_6.

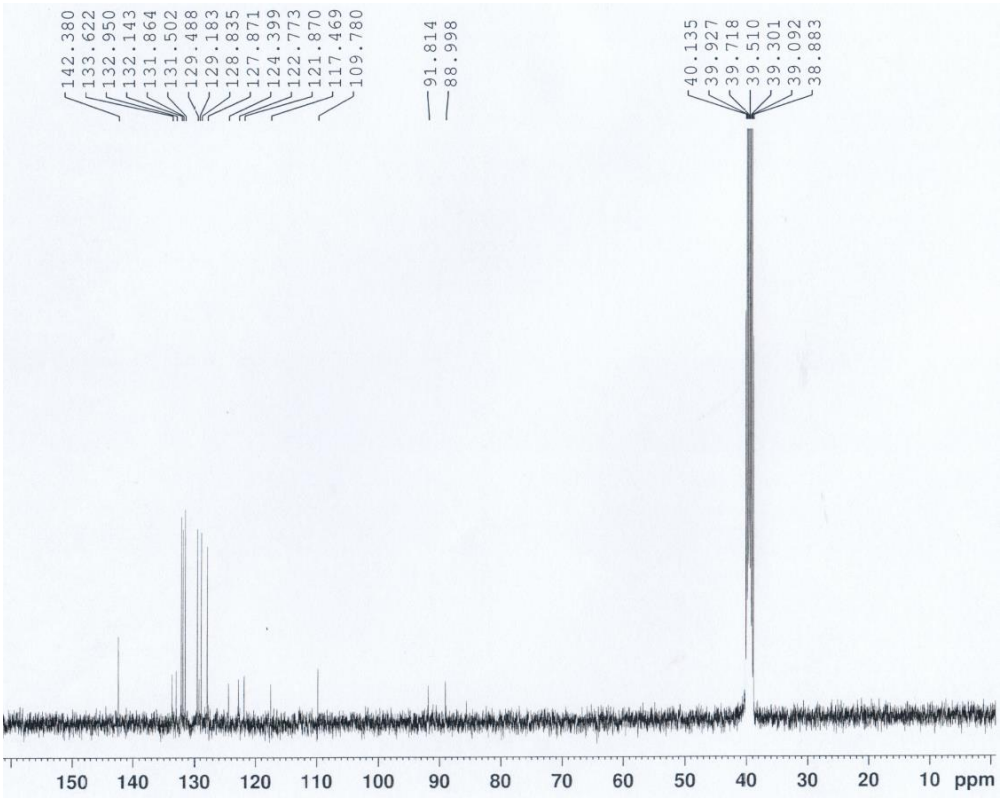

Figure S4. ^{13}C NMR spectrum of **3** in DMSO-d_6.

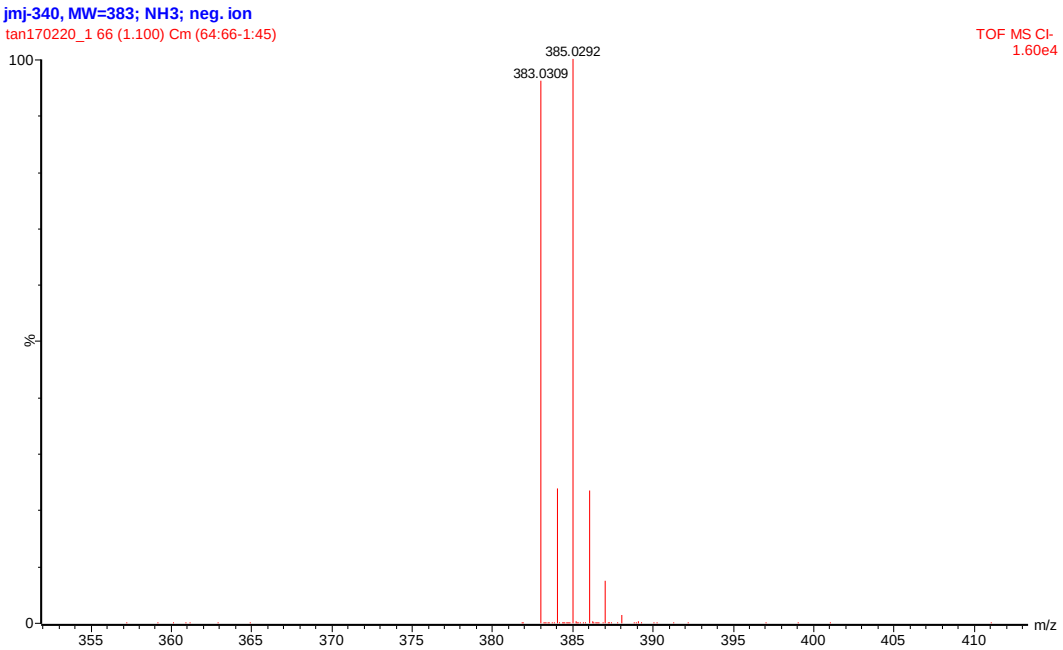

Figure S5. HR-MS spectrum of compound **3**.

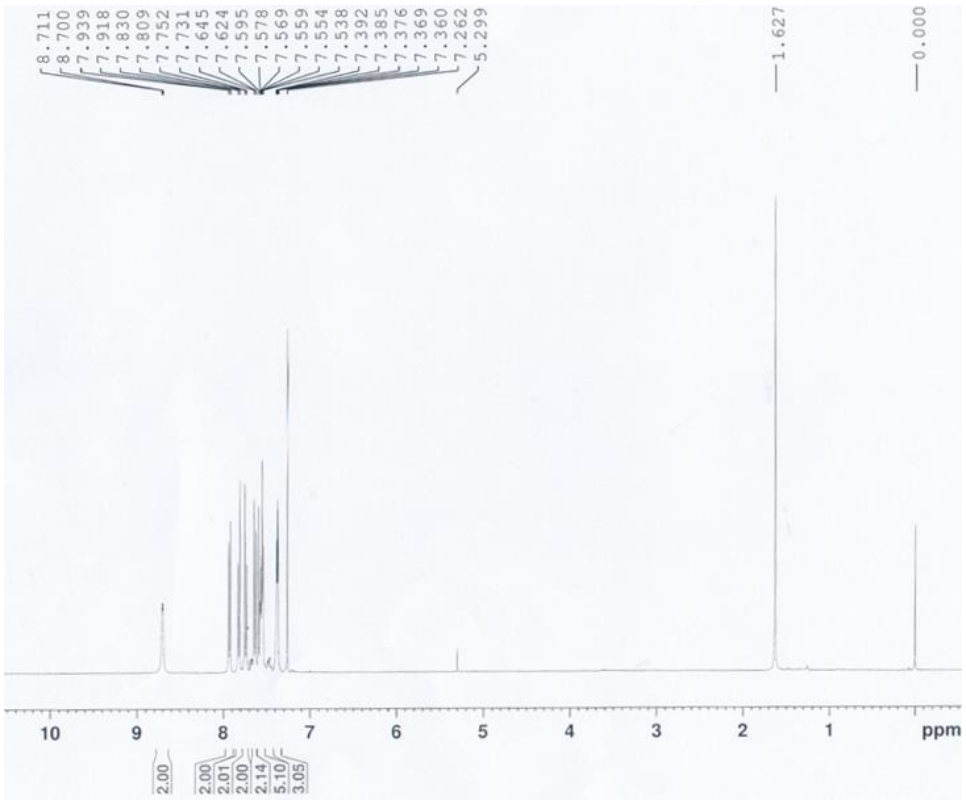

Figure S6. ^{1}H NMR spectrum of compound **2** in $CDCl_3$.

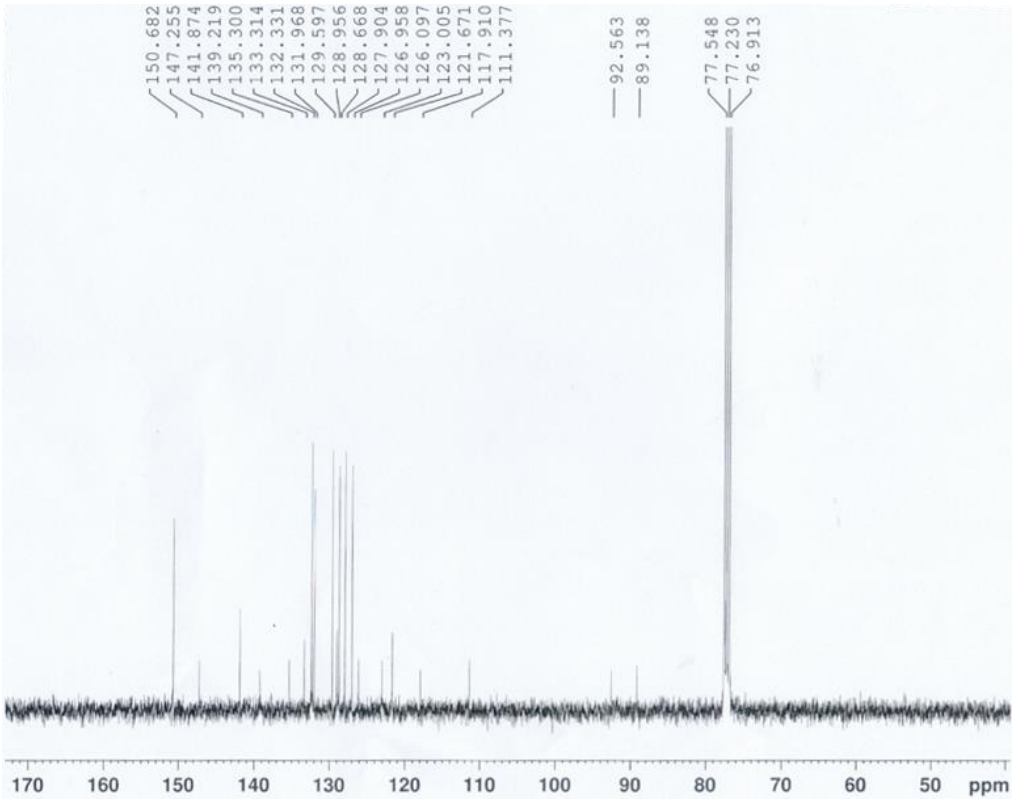

Figure S7. ^{13}C NMR spectrum of **2** in $CDCl_3$.

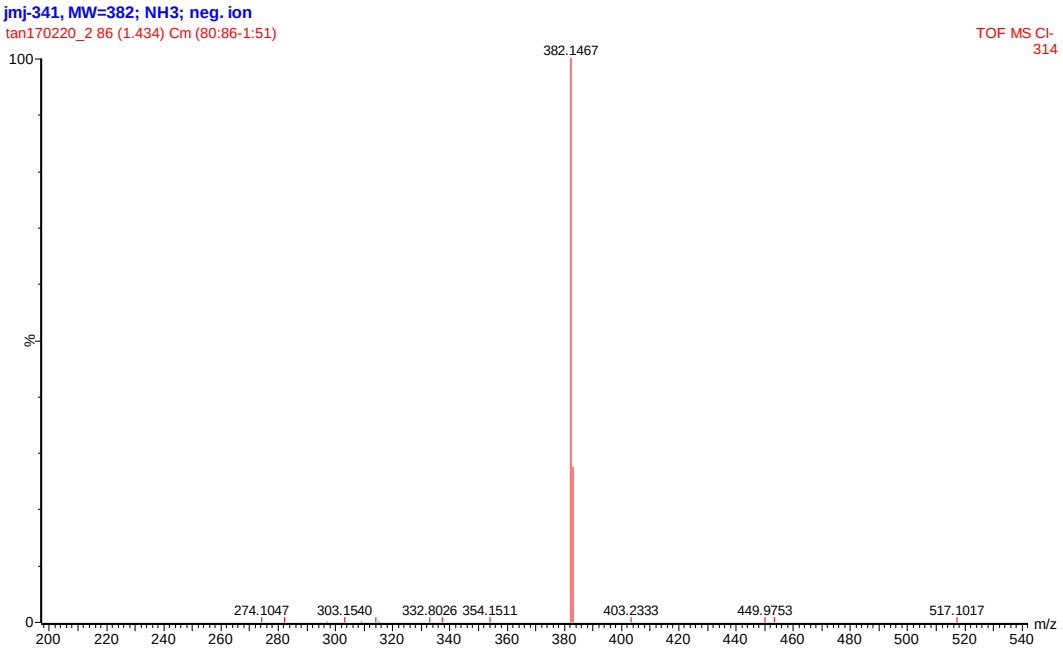

Figure S8. HR-MS spectrum of **2**.

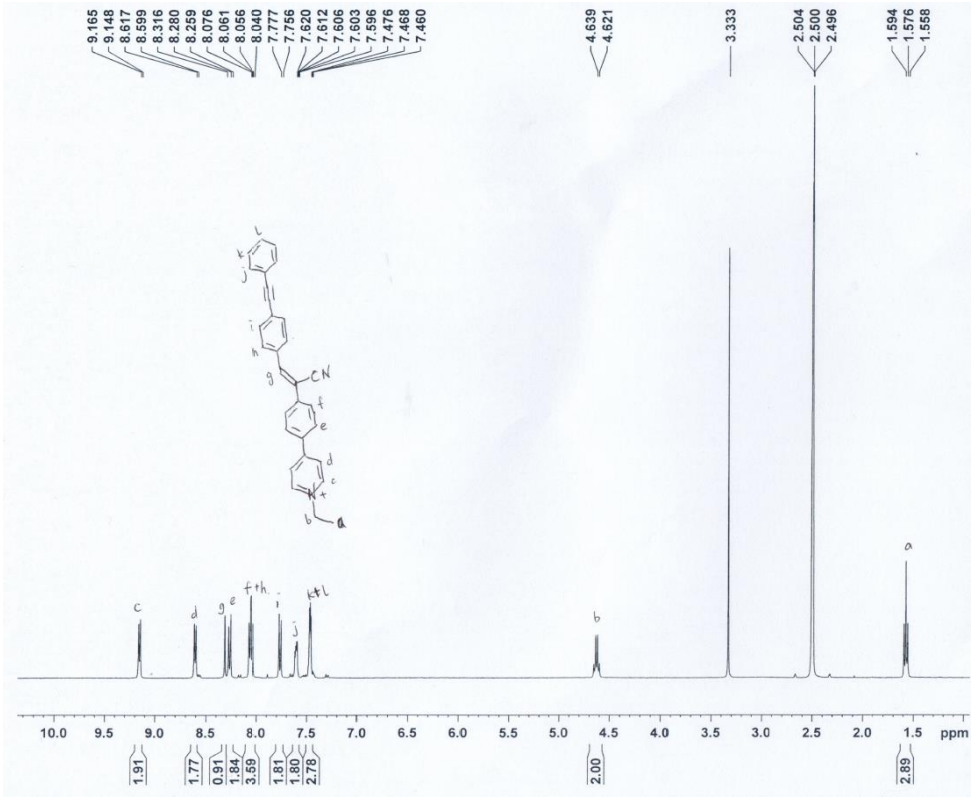

Figure S9. ^{1}H NMR spectrum of AIE-SRS-Mito in DMSO-d_6.

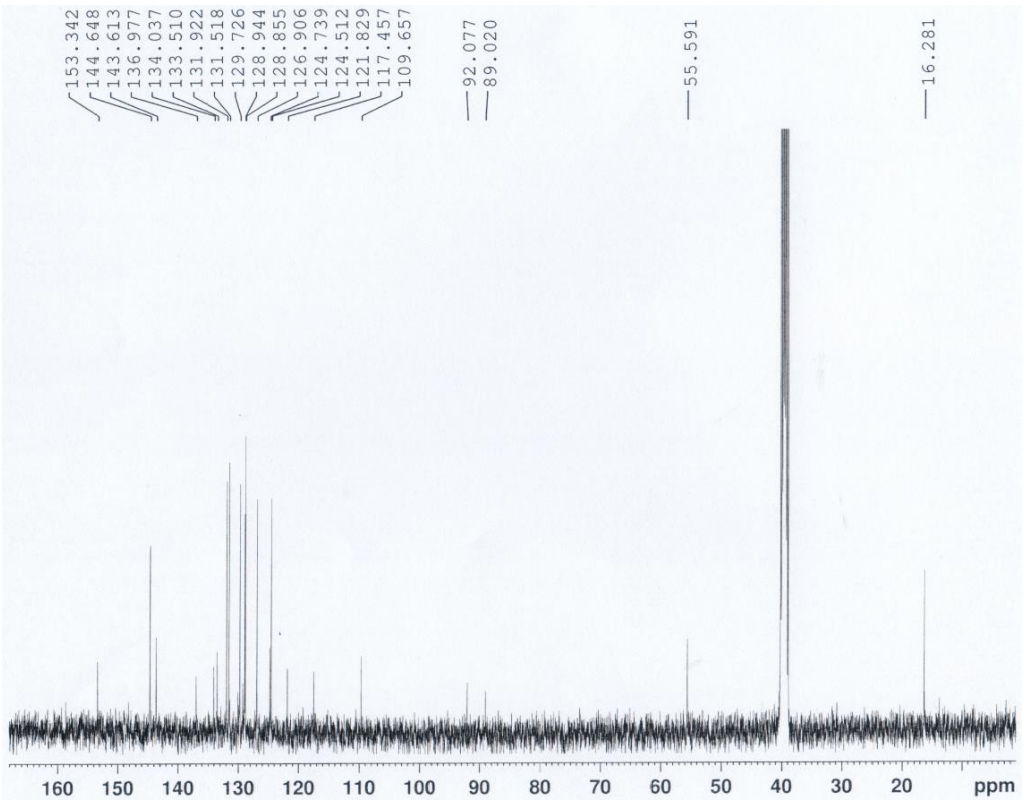

Figure S10. ^{13}C NMR spectrum of AIE-SRS-Mito in DMSO-d_6.

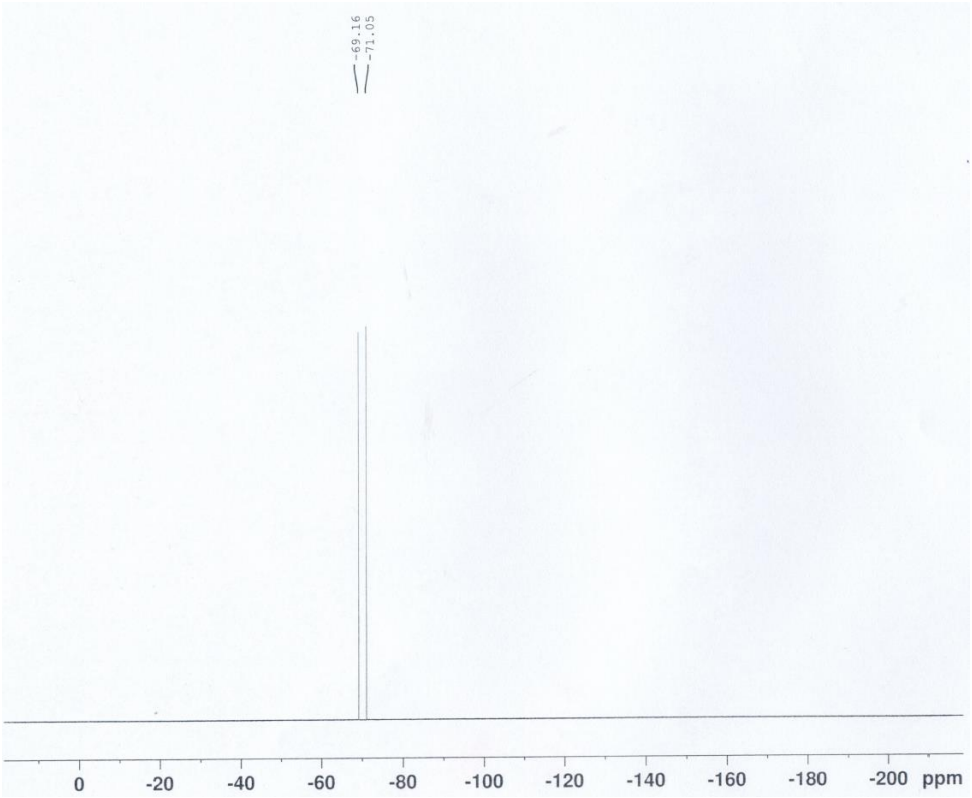

Figure S11. ^{19}F NMR spectrum of AIE-SRS-Mito in DMSO-d_6.

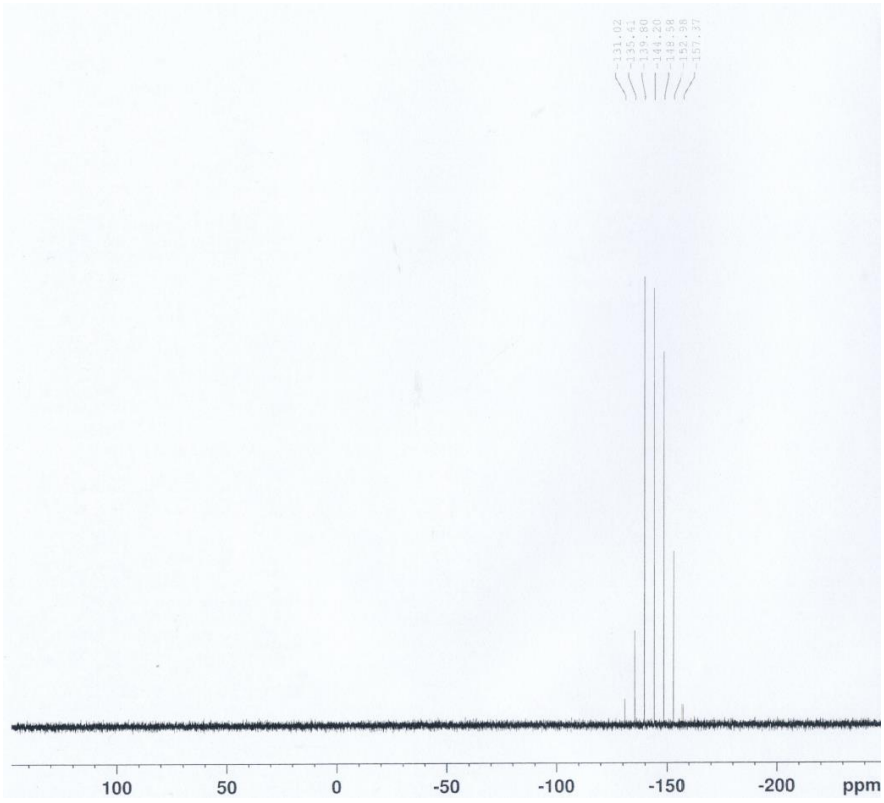

Figure S12. ^{31}P NMR spectrum of AIE-SRS-Mito in DMSO-d_6.

Figure S13. HR-MS spectrum cation of AIE-SRS-Mito.

Figure S14. HR-MS spectrum anion of AIE-SRS-Mito.

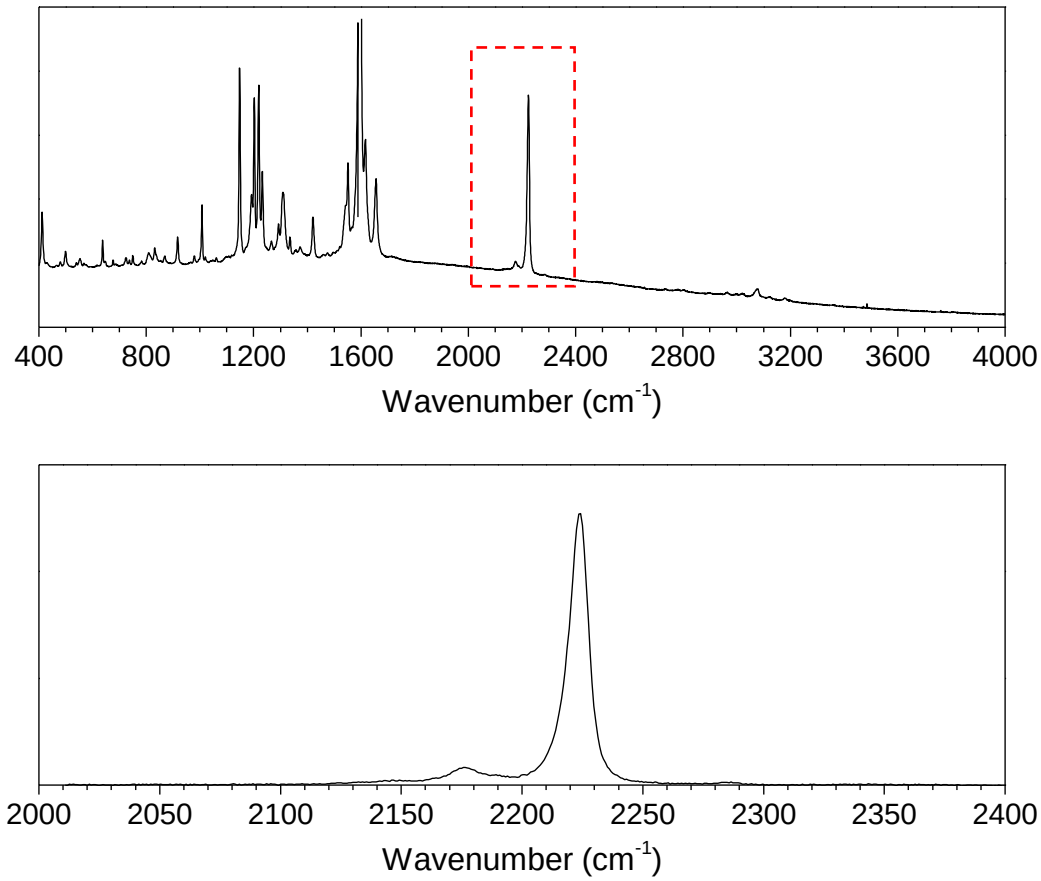

Figure S15. Spontaneous Raman spectrum of AIE-SRS-Mito in powder state. Peak wavenumber of alkyne: 2223.7 cm^{-1}.

Table S1. Photophysical properties of AIE-SRS-Mito and ASCP [a]

compound	λ_{abs}, nm	λ_{em}, nm	$\Phi_{soln.}$	Φ_{solid}	δ_{2PA}, GM
AIE-SRS-Mito	380	500	1.1%	13%	14.2
ASCP	450	650	0.2%	0.7%	61.9

[a] λ_{abs} and λ_{em} are the peak wavelength of 1PA and the emission spectra in DMSO. $\Phi_{soln.}$ and Φ_{solid} are the quantum yields in DMSO solution (1 mM) and solid state, respectively. Quantum yields Φ were measured under 400 nm excitation. δ_{2PA} are the two-photon absorption cross sections measured at 800 nm by using a femtosecond laser. 1 GM ≡ 10^{-50} cm^4 s/photon.

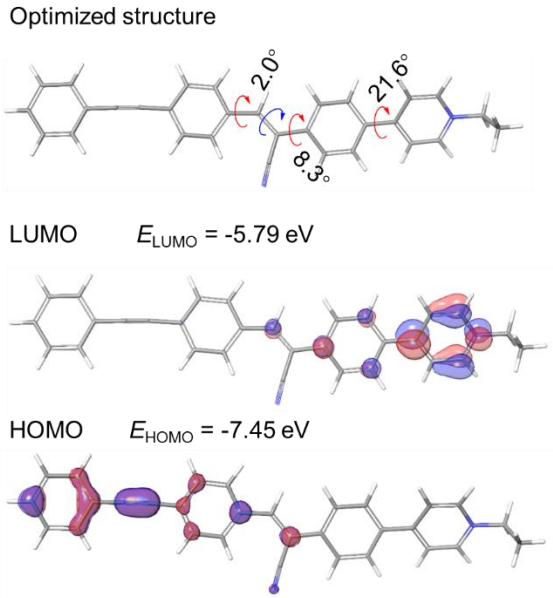

Figure S16. Optimized structure and the frontier orbitals (HOMO and LUMO) of AIE-SRS-Mito by DFT calculations at the base level of B3LYP/6-31G**.

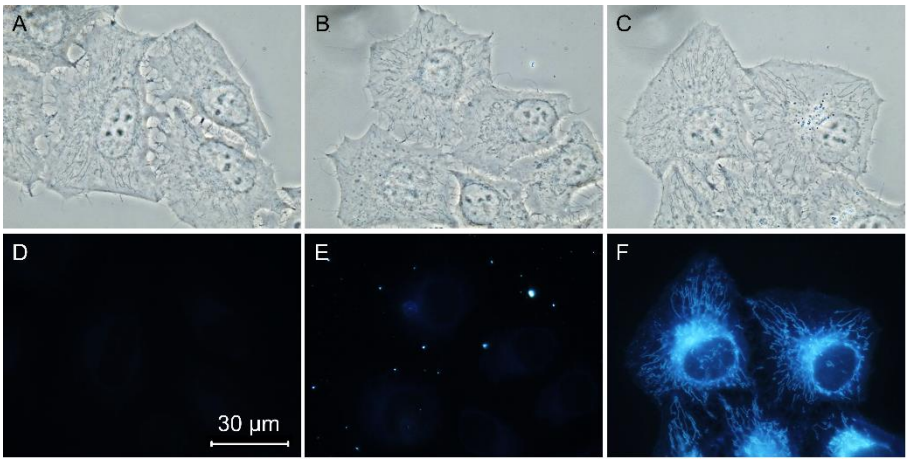

Figure S17. (A–C) Bright field (phase contrast) and (D–F) fluorescent images of HeLa cells stained with 5 μM of (A, D) **3**, (B, E) **2** and (C, F) AIE-SRS-Mito in culture medium for 20 min. Excitation wavelength: 330-385 nm.

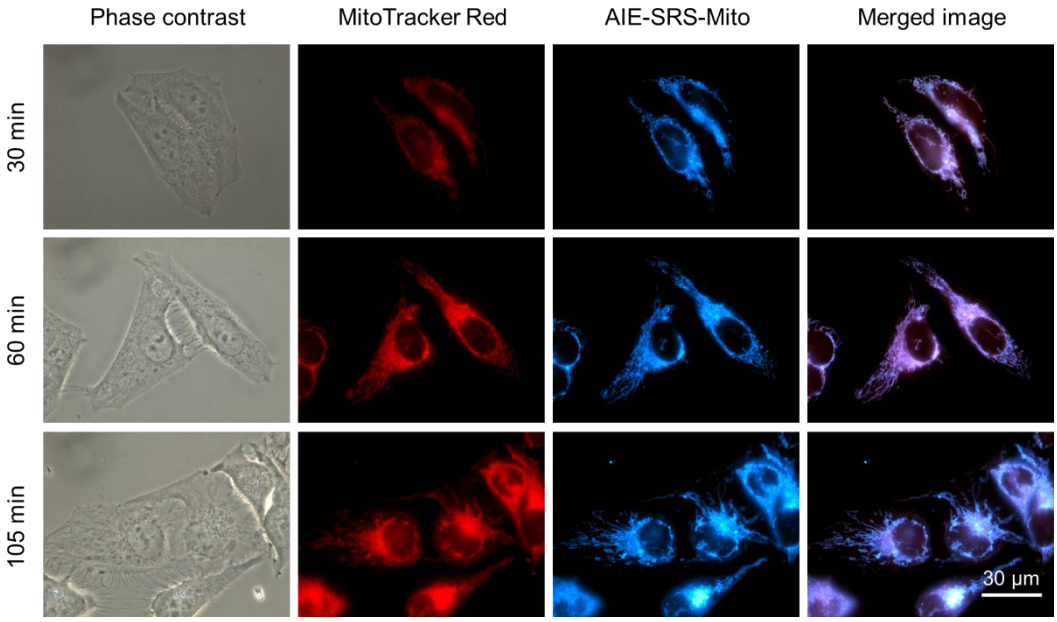

Figure S18. Bright field (phase contrast) and fluorescent images of HeLa cells co-stained with AIE-SRS-Mito (5 μM) and Mitotracker Red FM (100 nM) in cell medium for 30, 60 and 105 min. Excitation wavelength: 330-385 nm for AIE-SRS-Mito and 540-580 nm for MTR.

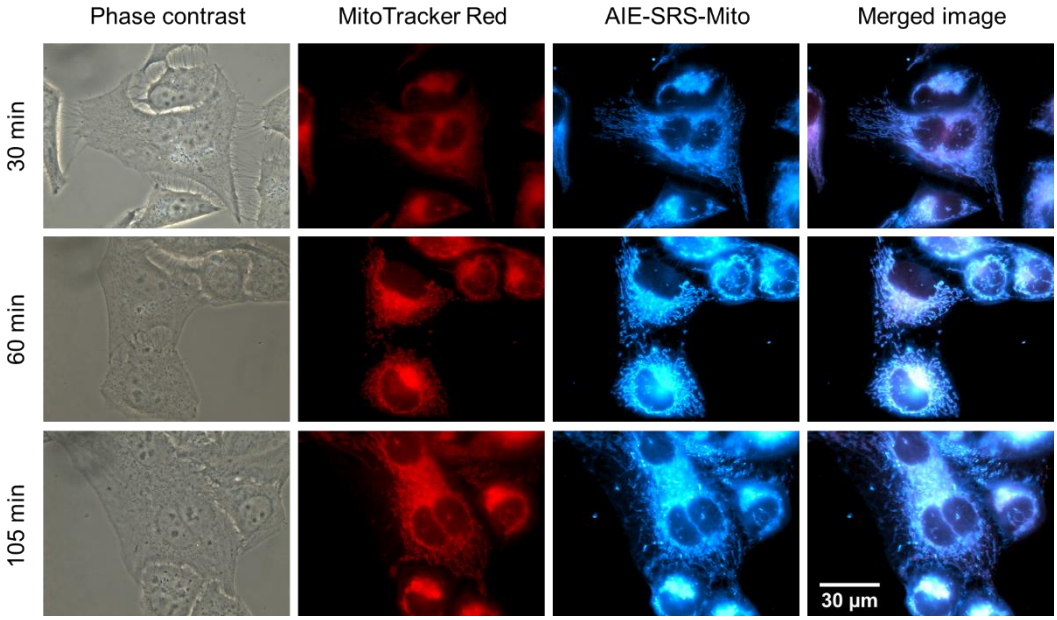

Figure S19. Bright field (phase contrast) and fluorescent images of HeLa cells co-stained with AIE-SRS-Mito (20 μM) and Mitotracker Red FM (100 nM) in cell medium for 30, 60 and 105 min. Excitation wavelength: 330-385 nm for AIE-SRS-Mito and 540-580 nm for MTR.

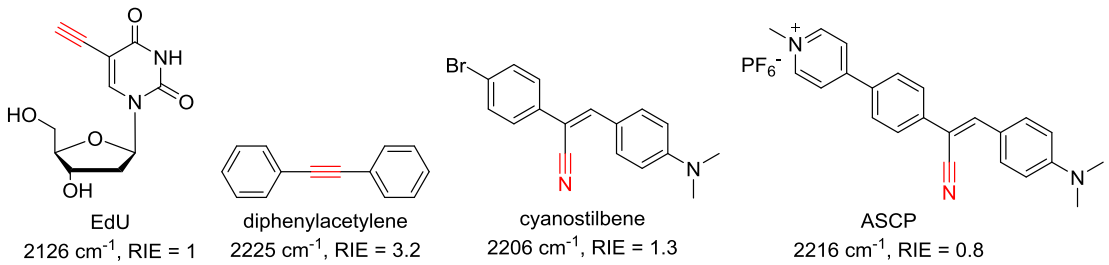

Figure S20. Chemical structures of EdU, diephenylacetylene, cyanostilbene and ASCP. Their SRS signal peak wavenumber and relative Raman intensity versus EdU (RIE) were noted.

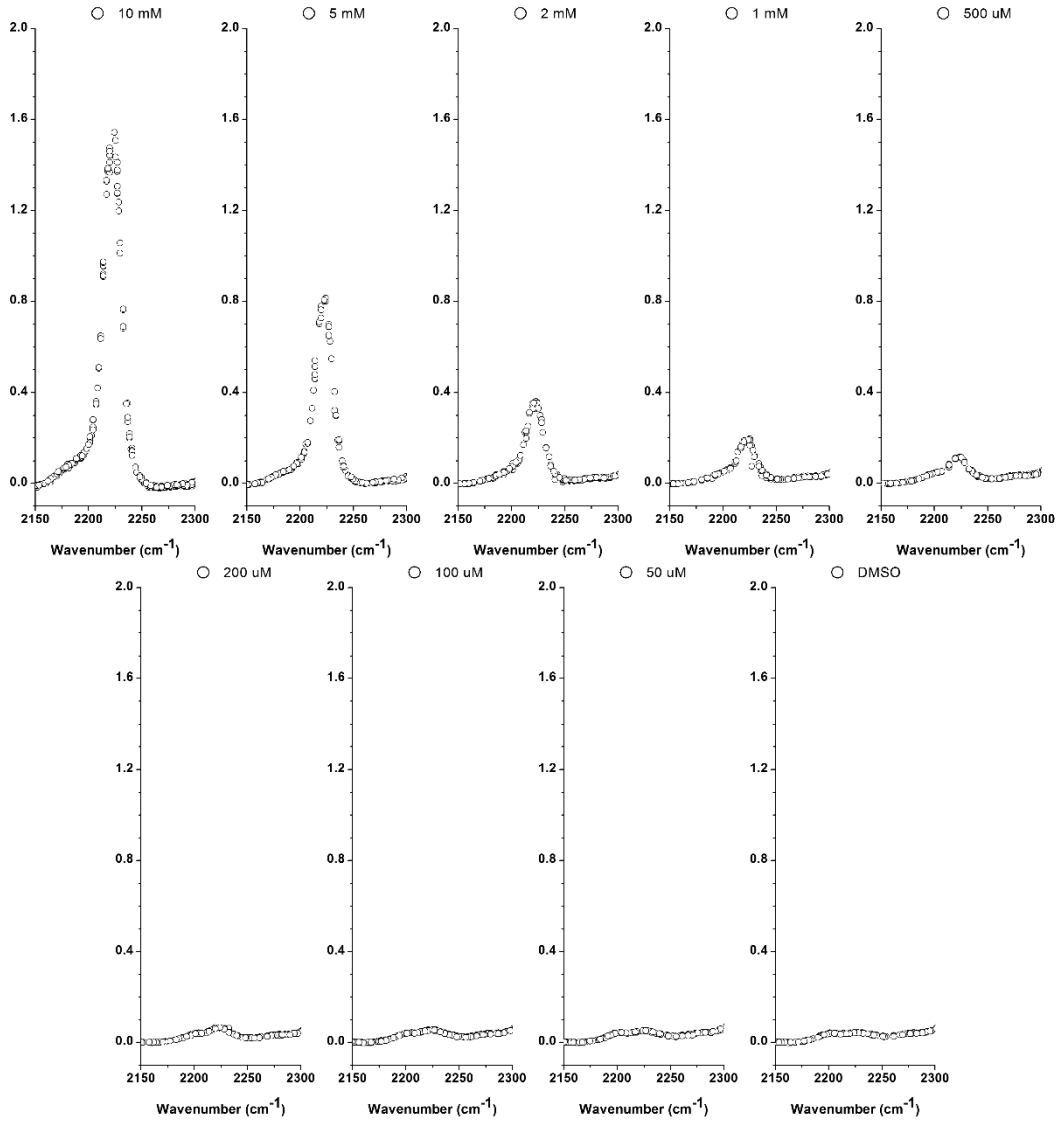

Figure S21. SRS spectra of AIE-SRS-Mito in DMSO at various concentrations.

Table S2. Determination of detection limit and quantification limit of AIE-SRS-Mito in DMSO.

DMSO (background)	Peak 838.8 nm (2222.5 cm^{-1})	Baseline 843.2 nm (2160.3 cm^{-1})	Peak - baseline
#1	0.161063302	0.118505223	0.042558079
#2	0.162277002	0.120281274	0.041995728
#3	0.162523314	0.121029595	0.041493719
#4	0.164496962	0.122210464	0.042286497
#5	0.166046059	0.123501479	0.04254458
		Average	**0.042175721**
		STDV	**0.000444986**

Detection limit = 3s/k = 0.000445*3/0.1567 = 8.5 μM
Quantification limit = 10s/k = 0.000445*10/0.1567 = 28.4 μM

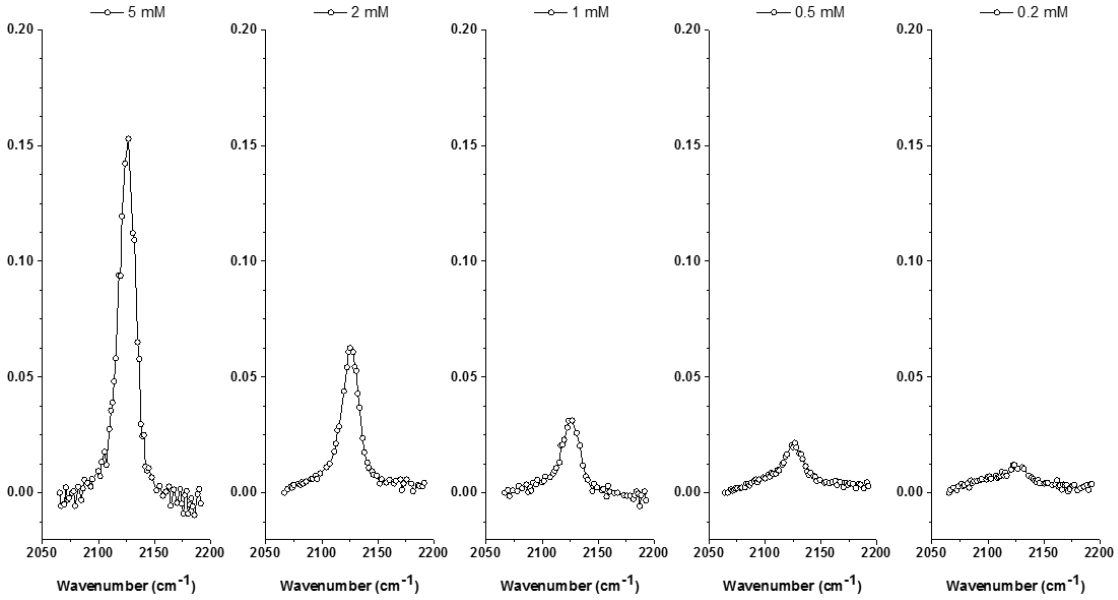

Figure S22. SRS spectra of EdU in PBS at various concentrations.

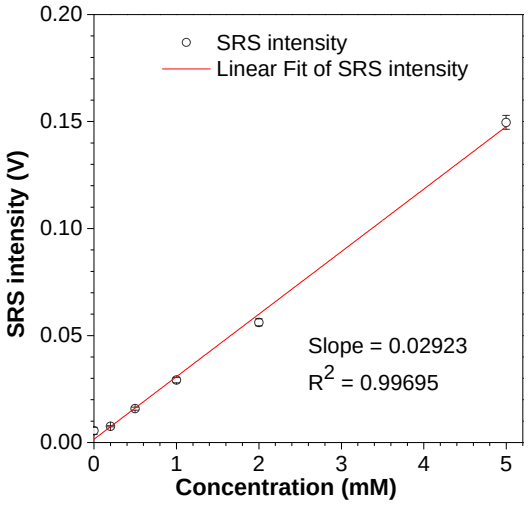

Figure S23. Change of SRS intensity I_{SRS} of EdU with different concentrations in PBS. The SRS intensity I_{ON} at 2125.2 cm^{-1} (on-resonance) and I_{OFF} at 2065.4 cm^{-1} (off-resonance) were used to calculate the genuine SRS signal intensity $I_{SRS} = I_{ON} - I_{OFF}$.

Table S3. Determination of detection limit and quantification limit of EdU in PBS.

PBS (background)	Peak 845.7 nm (2125.2 cm^{-1})	Baseline 850 nm (2065.4 cm^{-1})	Peak - baseline
#1	0.140509751	0.131428088	0.009081663
#2	0.140059449	0.134940946	0.005118503
#3	0.137466345	0.131030359	0.006435986
#4	0.141465071	0.137335966	0.004129105
#5	0.140660452	0.137188721	0.003471731
#6	0.140159434	0.135596515	0.00456292
#7	0.137106258	0.13040269	0.006703568
#8	0.139129117	0.134308383	0.004820735
#9	0.136636639	0.130791628	0.005845011
#10	0.136735891	0.13261102	0.00412487
		Average	**0.005429409**
		STDV	**0.001652991**

Detection limit = 3s/k = 0.001653*3/0.02923 = 169.7 μM
Quantification limit = 10s/k = 0.001653*10/0.02923 = 565.5 μM

Tips 1:
More importantly, we found that the signal quality from the solvent background also contributed to the detection limit. In our work, the detection limit was determined by

3s/k in which s is the standard deviation of background SRS signal from the solvent and k is the slope of the linear fitting. We found that the standard deviation for background SRS signal for DMSO (AIE-SRS-Mito solvent) was 0.000444986 and 0.001652991 for PBS (EdU solvent), respectively. The ratio is about 1/3.7, indicating that the background noise level for DMSO solutions was lower than PBS solutions. This explained that detection limit is 8.5 μM for AIE-SRS-Mito and 169.7 μM for EdU though their RIE difference is only 6-fold.

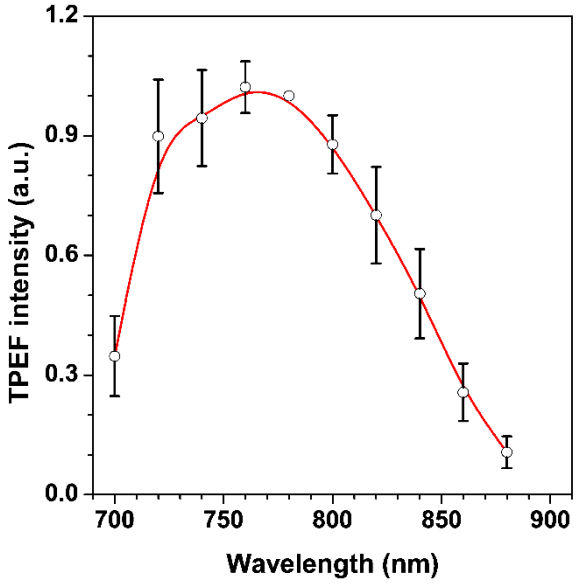

Figure S24. Plot of TPEF intensity versus excitation wavelength measured in live cells by using two-photon microscope with Ti:sapphire laser (laser power = 5 mW). HeLa cells were stained with 5 μM of AIE-SRS-Mito for 30 min. The intensity of the image of 780 nm was set to unity.

Tips 2:

The reasons for using different concentrations for 1P and 2P excitation experiments and the data for 2P excitation limited to 40% water fraction are as follows: the two experiments were conducted at different platforms for different purposes. We found that even at 10 μM concentration, the aggregates could be formed at high water fractions of >80 vol%. Higher dye concentration would also lead to more severe aggregation/precipitation, making the solution less transparent because of scattering from the aggregate suspension. The results presents in Figure 2C & 2D were from the 1P experiments that were carried out to demonstrate the AIE property of AIE-SRS-Mito using a commercial fluorometer. Therefore, certain aggregation in solution did not affect the study of AIE property. However, the results presented in Figure 4D are the study of polarity effect on fluorescence intensity and SRS signal intensity using the FL-SRS microscope system. Therefore, it is crucial to keep aggregation level as low as possible and to ensure the accuracy of quantitative SRS measurement. In consideration of the moderate SRS sensitivity (28.4 μM quantification limit) relative to fluorescence,

10 μM concentration was not suitable for this purpose. Thus, the solution of higher concentration (1 mM) and low water fractions (<40 vol%) were used in 2P experiment to avoid aggregation and ensure good quality SRS signal.

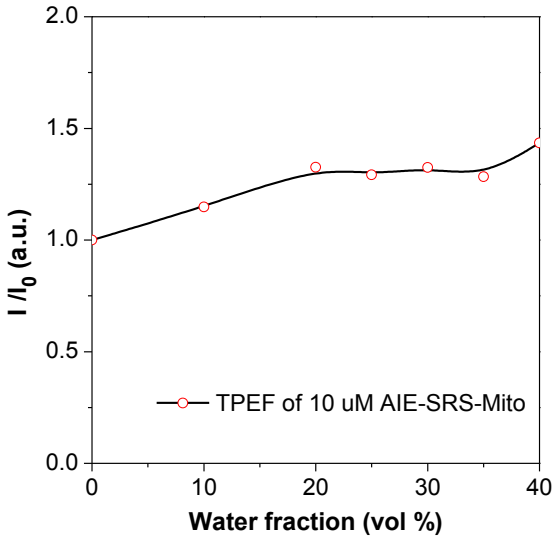

Figure S25. TPEF intensity of AIE-SRS-Mito (10 μM) in DMSO-water mixtures with different water fractions. Excitation wavelength: 780 nm for AIE-SRS-Mito (laser power: 10 mW).

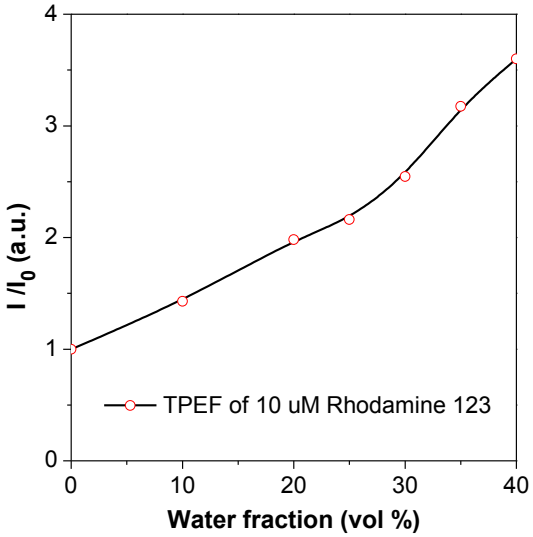

Figure S26. TPEF intensity of Rhodamine 123 (10 μM) in DMSO-water mixtures with different water fractions. Excitation wavelength: 900 nm for Rhodamine 123 (laser power: 6 mW).

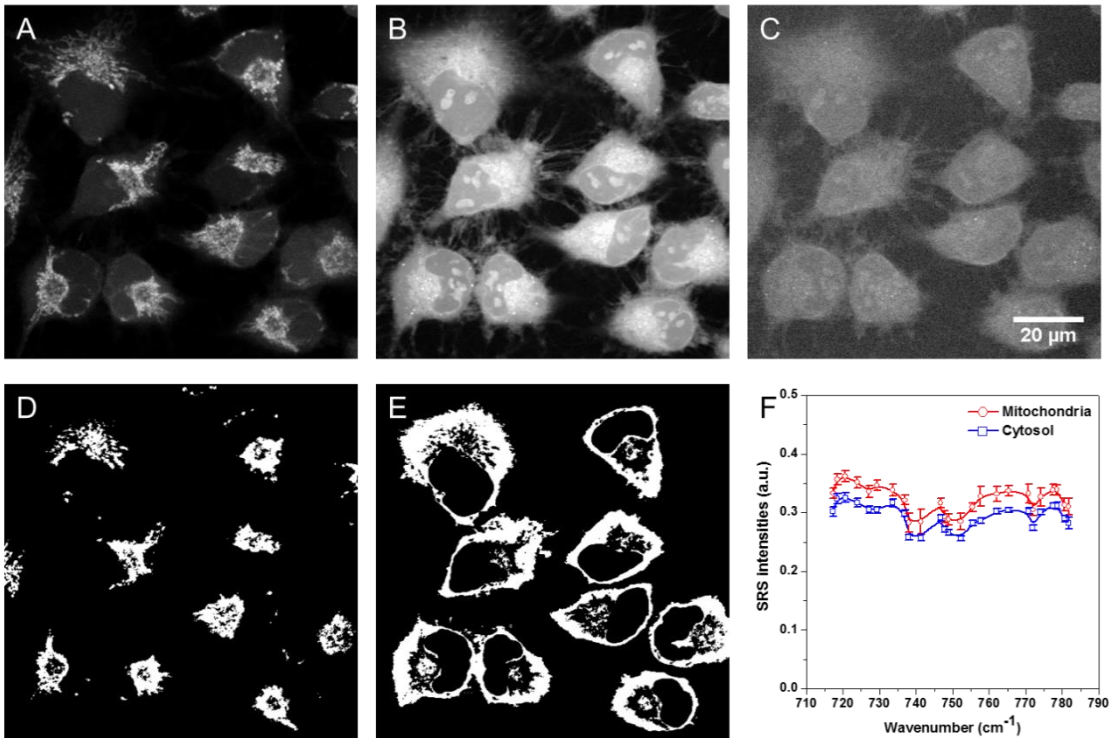

Figure S27. Image-guided SRS spectroscopy in the fingerprint region from 710 ~ 790 cm^{-1} using the FL-SRS system. (A) TPEF image of NADH in HeLa cells. Excitation wavelength of fs laser: 740 nm; emission filter: Chroma HQ440/80. (B) SRS image of protein at 2,950 cm^{-1}. (C) SRS image at 752 cm^{-1}. (D) Mask of mitochondrial compartment extracted from NADH TPEF image. (E) Mask of cytosolic compartment extracted from NADH TPEF and SRS protein images. (F) SRS spectra of mitochondria and cytosol recovered from the mitochondrial and cytosolic compartments. Data analysis was conducted on individual cells (n = 9).

Note: Nicotinamide adenine dinucleotide (NADH) is a metabolic coenzyme and an endogenous fluorophore in cells. The concentration of NADH in mitochondria is much higher than other cellular compartments. Therefore, it is considered as an endogenous fluorescence marker of mitochondria. In this experiment, instead of using any mitotracker we used NADH TPEF imaging to locate the mitochondria in cells to avoid any possible artifact in the measurement of mitochondrial SRS spectrum. The NADH TPEF images were recorded before and after the SRS spectroscopy of mitochondria in fingerprint region from 710 ~ 790 cm^{-1}. Two NADH TPEF images were carefully compared to ensure no movement of mitochondria during the SRS spectroscopy. In general, the signal quality of each pixel in the hyperspectral SRS (hsSRS) images was not sufficiently high to obtain a reliable Raman spectrum. For accurate analysis of the SRS signals in cells, we divided the image of a cell into the compartments of mitochondria and cytosol. We summed up the signals in two compartments to generate high-quality SRS spectra of mitochondria and cytosol. The details of this image-guided spectroscopy method were described in previous work (Li, D.; Zheng, W.; Qu, J. Y., Time-resolved spectroscopic imaging reveals the fundamentals of cellular NADH fluorescence. *Optics letters* **2008,** *33* (20), 2365-2367). Briefly, we used the threshold based edge detection to localize the mitochondrial areas in the NADH TPEF image and

generate a mask of mitochondrial compartment (Fig. S27D). The protein image (Fig. S27B) provides clear locations of nuclei and was used to define the nuclear areas. The mask of cytosolic compartment (Fig. S27E) was obtained by subtracting the cell image from mitochondrial and nuclear compartments. The SRS spectra of mitochondria and cytosol shown in Fig. S27F are the summed-up spectra from mitochondrial and cytosolic compartments, respectively.

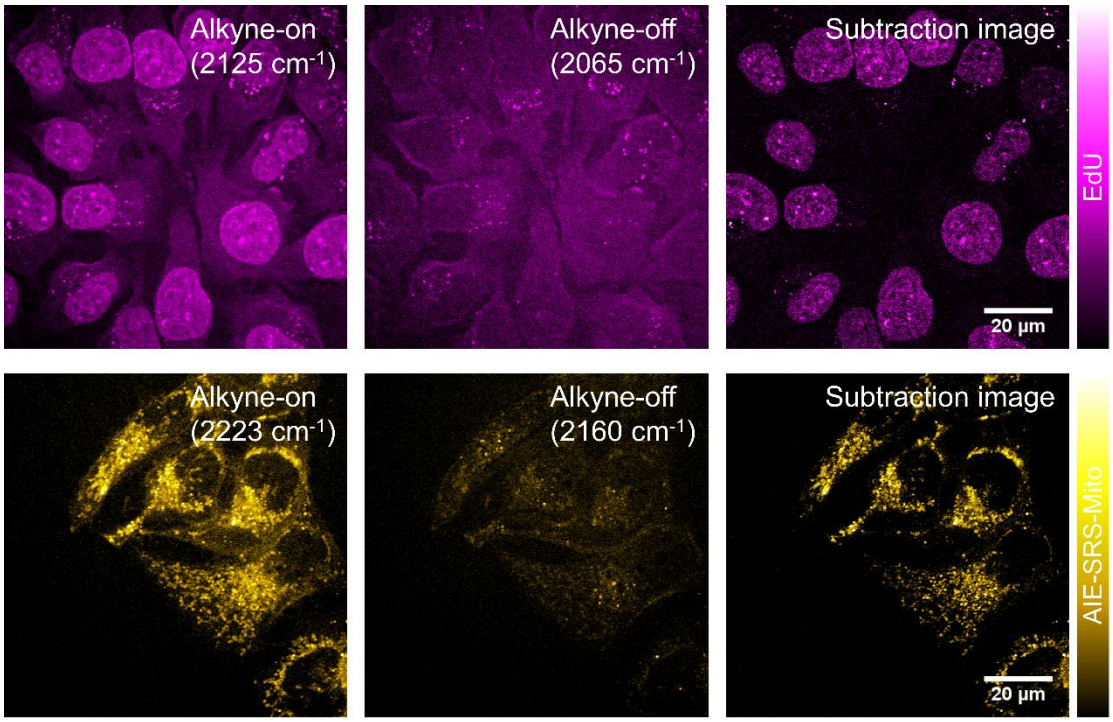

Figure S28. A pair of "alkyne-on" and "alkyne-off" images were acquired and subtracted to reconstruct the final image. This IM-SRL method suppresses the non-Raman backgrounds, including XPM, TA and thermal lensing effects.

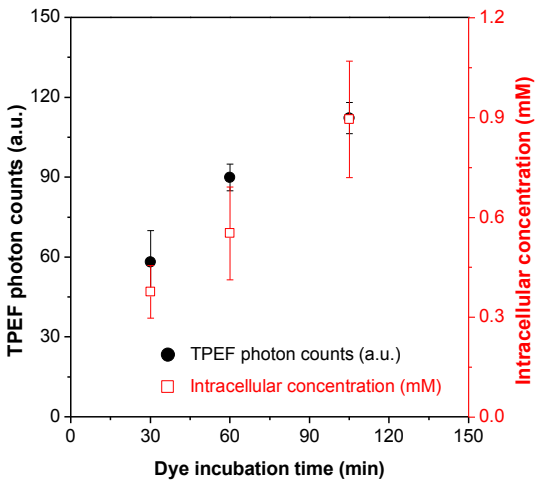

Figure S29. The averaged fluorescence intensity and averaged SRS intensity of HeLa cells stained with 20 μM AIE-SRS-Mito for 30 min, 60 min and 105 min. The fluorescence intensity and SRS intensity were averaged over a single cell. Under each

condition, more than 10 cells were analyzed.

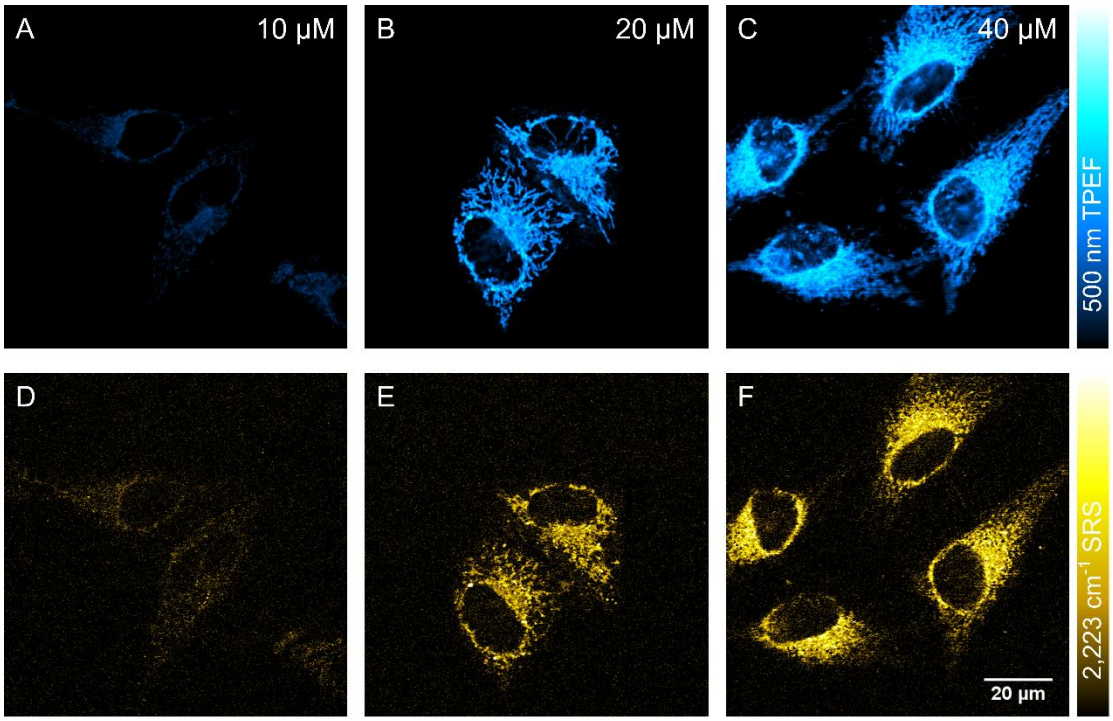

Figure S30. (A–C) Fluorescent images and (D–F) SRS images of HeLa cells stained with (A, D) 10 μM, (B, E) 20 μM and (C, F) 40 μM of AIE-SRS-Mito for 30 min.

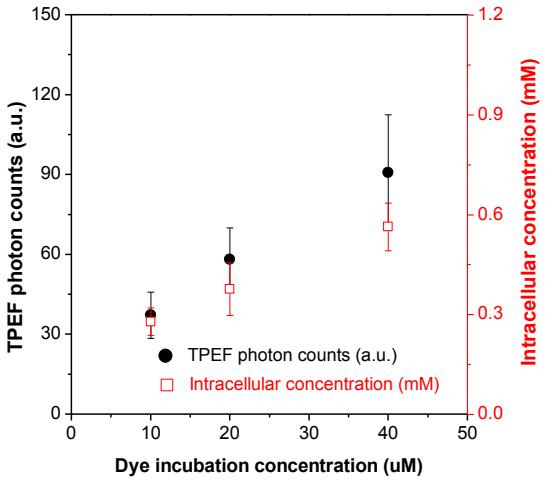

Figure S31. The averaged fluorescence intensity and averaged SRS intensity of HeLa cells stained with 10, 20 40 μM AIE-SRS-Mito for 30 min. The fluorescence intensity and SRS intensity were averaged over a single cell. Under each condition, more than 10 cells were analyzed.

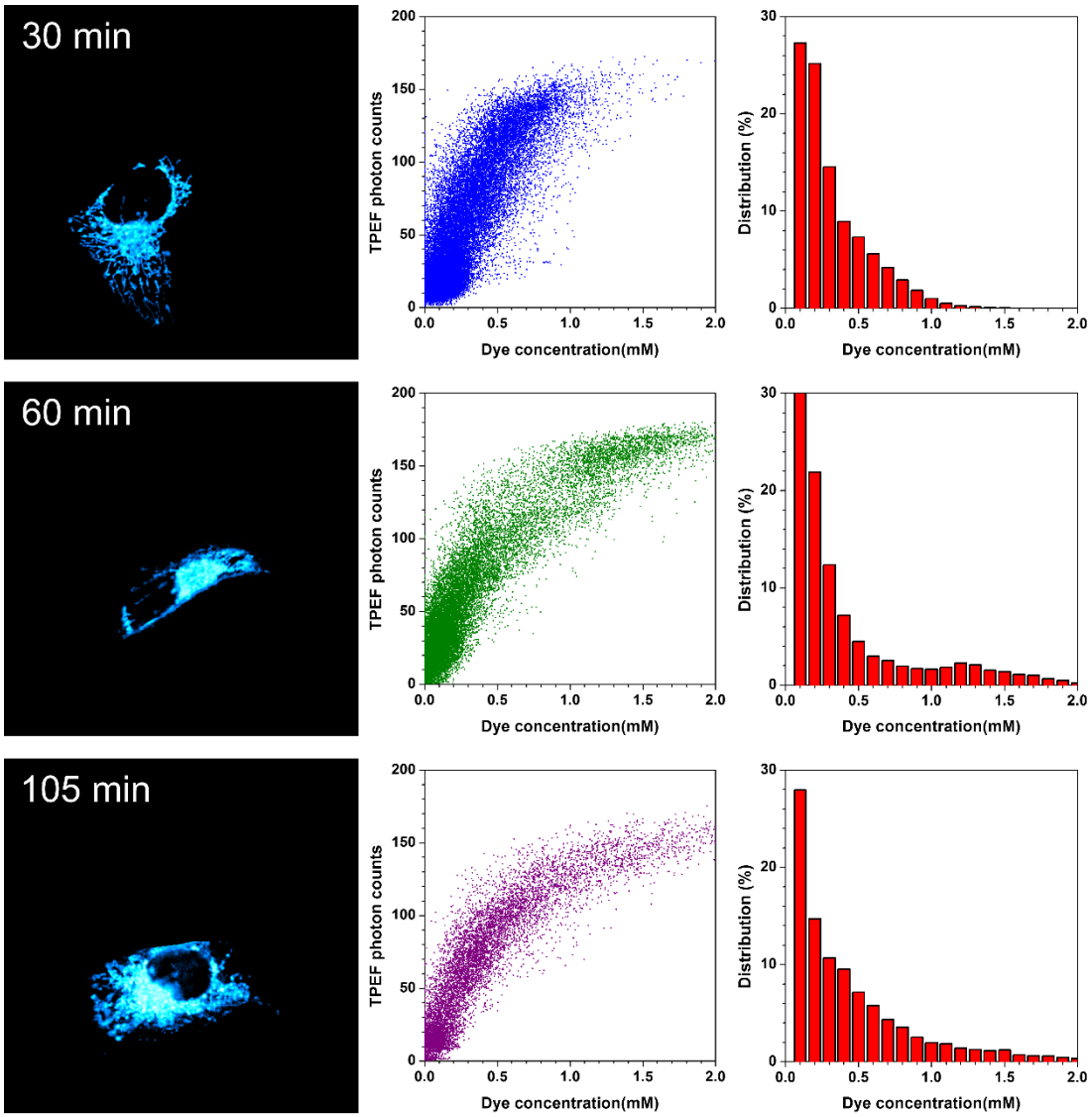

Figure S32. Representative cell images (first column), plot of colocalization of fluorescence intensity and dye concentration (second column), and histogram of dye concentration (third column) of HeLa cells stained with 20 μM AIE-SRS-Mito for 30, 60 and 105 min, respectively.

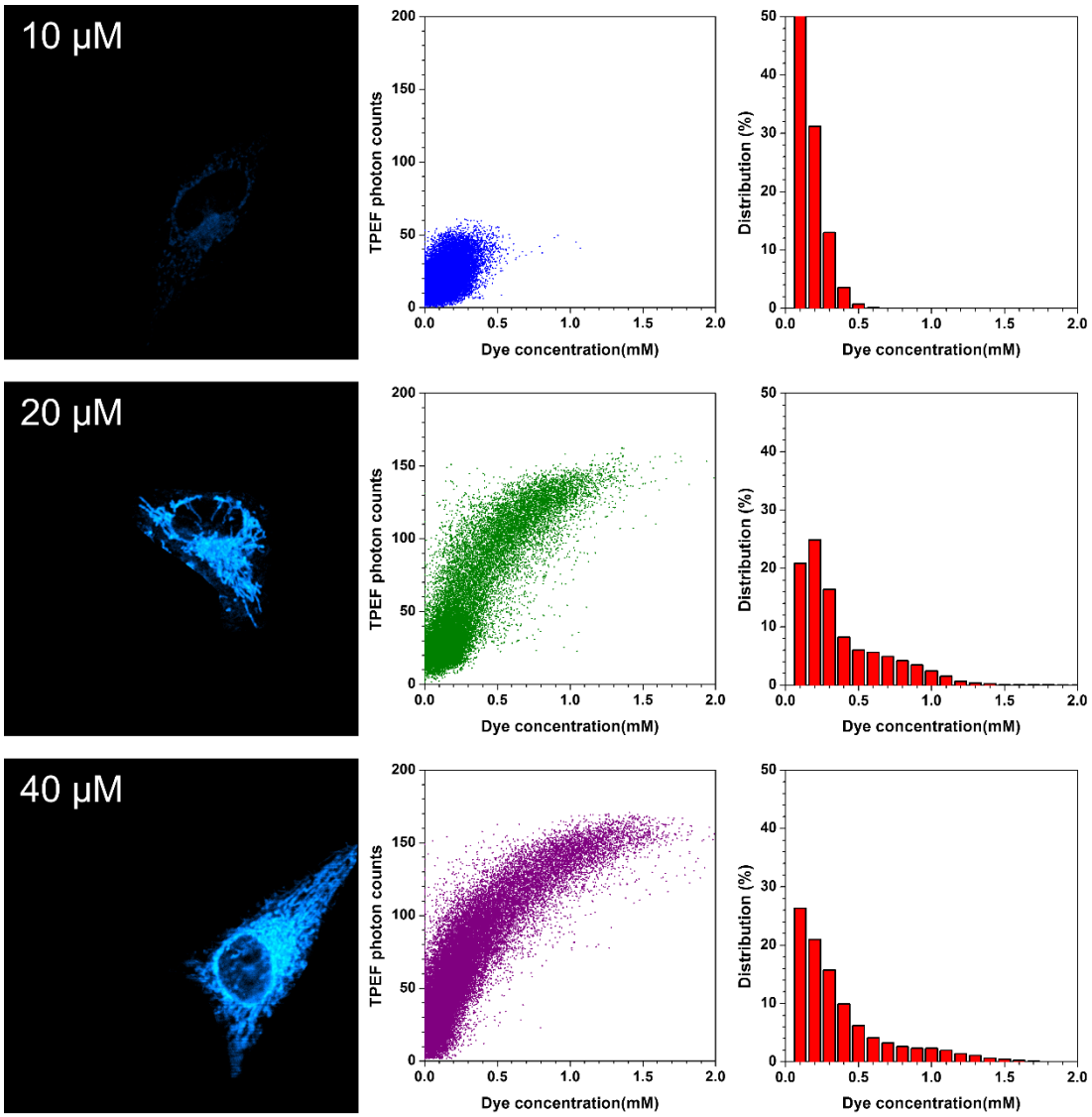

Figure S33. Representative cell images (first column), plot of colocalization of fluorescence intensity and dye concentration (second column), and histogram of dye concentration (third column) of HeLa cells stained with 10, 20, 40 μM AIE-SRS-Mito for 30 min, respectively.